The use of binary polymeric networks in stabilising polyethylene oxide solid dispersions

Jones, D. S., Tian, Y., Li, S., Yu, T., Abu Diak, O. A., & Andrews, G. P. (2016). The use of binary polymeric networks in stabilising polyethylene oxide solid dispersions. Journal of Pharmaceutical Sciences, 105(10), 3064–3072. DOI: 10.1016/j.xphs.2016.06.004

Published in:
Journal of Pharmaceutical Sciences

Document Version:
Peer reviewed version

Queen's University Belfast - Research Portal:
Link to publication record in Queen's University Belfast Research Portal

The use of binary polymeric networks in physical stabilization of polyethylene oxide solid dispersions

David S. Jones, Osama A. Abu-Diak, Yiwei Tian, Gavin P. Andrews.

The Drug Delivery and Biomaterials Group, School of Pharmacy, Medical Biology Centre, Queen's University, 97 Lisburn Road, Belfast. BT9 7BL, Northern Ireland, UK

Abstract

The objective of this study was to investigate the role of amorphous domain of polyethylene oxide (PEO), a semicrystalline polymer, on the stability of drug/PEO solid dispersion. Molecular dispersion of drugs within hydrophilic low molecular weights PEOs (solid solution) has been demonstrated as a viable approach to enhance the dissolution properties and hence the oral bioavailability of poorly soluble drugs. In this system, the drug molecules are dissolved within the amorphous domain of the polymer and a miscible amorphous drug/polymer combination can result in a decrease of the polymer crystallinity, and hence increasing its amorphous fraction. This may result in increasing the drug solubility in the polymer hence affecting the stability of drug/polymer solid dispersion system. PEO is a highly crystallisable semi-crystalline polymer in natural and a rapid decrease in the amorphous fraction of the polymer may occur immediately after hot-melt extrusion resulting a forced migration of amorphous drug into nearby amorphous region. Thus, the actual concentrations of the drug within PEO solid dispersion were much higher than the concentration that we intended. Therefore, we are proposing a novel method of stabilising the amorphous drug/PEO solid dispersion by stabilising the amorphous region of PEO using another amorphous polymer. Inclusion of a miscible polymer that can increase the glass transition (*Tg*) of PEO (antiplasticization) or/and form strong inter-polymer interactions was used to enhance the stability of the amorphous PEO. In this study, the effects of inter-polymer interactions and miscibility between PEO and an amorphous polymer of high *Tg*, Eudragit® S100, on the stability of the amorphous PEO and consequently the PEO/drug celecoxib (CX) solid dispersion was studied. Hot-melt extrusion (HME) was used to prepare different ratios of binary polymer blends of PEO/S100 (70/30, 50/50 and 30/70 w/w) and ternary solid dispersion systems containing pre-defined drug loading within the PEO/S100 polymer blends. Results from differential scanning calorimetry (DSC) and dynamic mechanical thermal analysis (DMTA) suggested a great miscibility between PEO and S100 polymer blends particularly in the 50/50 ratio. After immediately HME, single *Tg* was observed in all ternary systems that increase with increasing S100 amount (antiplasticization). The completely absence of PXRD crystalline Bragg's peaks also suggested the full amorphous CX/polymer solid dispersion has been produced. Upon storage, CX crystallized rapidly from the CX/PEO (30/70)

system within 3 days at 40°C and 75% RH, whereas it remained stable without crystallization up to 4 weeks within CX/(PEO/S100) 30/(50/50) system. Interestingly, both the stability of the amorphous PEO and CX were greater in the ternary system containing the polymer blend at 50/50 ratio than other systems. Despite of the lower *Tg* of 30/(50/50) system than 30/(30/70) one, the former was more stable. This indicates that the antiplasticization effects by Eudragit® S100 were not the predominant mechanism in such stabilization and also highlights the role of the inter-polymer interactions in stabilizing the amorphous PEO and consequently the drug dissolved in the amorphous region of PEO. FTIR studies confirmed the presence of hydrogen bonding between the carboxyl groups of Eudragit® S100 and the oxygen ether of PEO after HME. The strength of these inter-polymer interactions appeared to the highest in the systems containing a polymer blend of 50/50 ratio comparing to other systems. These findings suggest that the inter-polymer hydrogen bonding between PEO and Eudragit® S100 was the main reason for stabilizing the amorphous PEO, and consequently the stability of CX/PEO solid dispersion system.

Keywords: solid dispersion; hot-melt extrusion; polymer blends; inter-polymer interactions; Flory-Huggins theory

1.0 Introduction

The use of combinatorial chemistry and high-throughput screening has resulted in a significant number of poorly-water soluble drugs within pharmaceutical development pipelines (Lipiniski *et al*., 2001; Lindenberg *et al*., 2004). More than 40% of marketed drugs have been estimated as either poorly soluble or water insoluble (Dubin, 2005). It is well accepted that addressing this problem is one of the most significant challenges being faced within the development of oral drug products (Leuner and Dressman, 2000, Sarnes et al., 2014). The slow drug dissolution rate and low drug solubility in the gastro-intestinal fluids may result in incomplete and variable bioavailability. One of the enabling strategies that can be used to overcome this problem is increasing the drug solubility or/and dissolution rate via the development of solid dispersions (Serajuddin, 1999). The drug can either be molecularly dispersed, dispersed as an amorphous form or as small crystals in an inert hydrophilic carrier (Chiou and Reigelman, 1971). Often, amorphous drugs have higher solubility than their crystalline counterparts (Hancock and Zografi, 1997). Although, the development of solid dispersions continues to be explored within the research area, the commercial success of dosage forms containing amorphous drugs is still limited due to poor physical stability and scale up problems (Serajuddin, 1999; Bikiaris, 2011). The low physical stability of amorphous drugs and their tendency to re-crystallize rapidly negate their solubility advantage. Polymers used in solid dispersions can stabilize amorphous drugs either by their anti-plasticization effects (Van den Mooter *et al*., 2001) or by their strong interactions with the drugs (Huang *et al*., 2008; Andrews *et al*., 2010a, Abu-Diak et al, 2011, Abu-Diak et al., 2012). Therefore, the rational selection of polymeric excipients is very important in producing stable amorphous solid dispersion (Tian et al, 2013).

Solid dispersions can generally be prepared using melt or solvent methods. In the solvent method, the drug and carrier are dissolved in a mutual solvent followed by solvent removal. In melting method, drug/carrier solid dispersions are prepared by co-melting/cooling. The problems associated with the organic solvents e.g. toxicity, safety hazards and solvent residuals make melting the method of choice despite of the potential problem of thermal degradation of drugs and carriers. Over the last decade, hot-melt extrusion (HME) has gathered renewed interest, particularly with

regard to production of solid dispersions (Albers *et al*., 2009; Lakshman *et al*., 2008; Miller *et al*., 2008, Tian et al., 2014).

Polyethylene oxide (PEO) is a semicrystalline non-ionic thermoplastic polymer exhibiting a low melting point, rapid solidification rate and low toxicity making it ideal for HME and formation of amorphous solid dispersion (Zhang and McGinity, 1999). Due to their hydrophilic character and ability to form solid dispersions, lower molecular weight PEOs have been widely used as carriers to enhance the solubility/dissolution properties of poorly soluble drugs (Li *et al*., 2006; Ozeki *et al*., 1997; Schachter *et al*., 2004). Melting of PEO followed by solidification upon cooling may decrease PEO crystallinity, and hence increase the amorphous PEO fraction (Prodduturi *et al*., 2005). Molecular dispersions of drugs within semicrystalline polymers (solid solutions) can be formed by dissolution of drug molecules within the amorphous domain of these polymers rather than in the crystalline fraction (Janssens *et al.*, 2008, Qing *et al.*, 2010, Abu-Diak *et al*., 2012). In previous studies, it has been shown that the dissolution of ketoprofen within the amorphous domains of PEO was resulted in the formation of solid solutions (Schachter et al., 2004). Additionally, drug/polymer miscibility may result in a decrease of PEO crystallinity thus leading to dissolution of larger amount of drug. This effect has been extended to other drugs compounds with a more recently study by Janssens *et al* (2008) confirming that the crystallinity of a polymeric carrier significantly influences the solubility of itraconazole (Janssens et al., 2008). However, PEO is also a highly crystallisable and hence a rapid decrease in its amorphous fraction can occur with time (Qing *et al.*, 2010). This decreases the drug solubility and resulted in a phase separation and drug re-crystallization (unstable solid solutions) despite the apparent high solubility/miscibility of drug in the amorphous region of PEO (Schachter *et al*, 2004, Li *et al*., 2006). Therefore, stabilizing the amorphous fraction of PEO may result in increasing the stability of drug/PEO solid dispersions.

The miscibility and interactions within binary PEO-based polymer blends have been studied extensively in polymer sciences (Kuo and Chang, 2001; Brus *et al*., 2000, Chu and Wu, 2000; Miyoshi *et al*., 1996). PEO can act as a proton acceptor through the oxygen atom of ethylene oxide monomer (Robeson *et al*., 1981). It has been reported that PEO can form miscible polymer blends, complexes, through formation of specific hydrogen bonding interactions with polymers containing proton donor

groups e.g. poly(acrylic acid) (PAA) (Smith *et al.*, 1959), poly(methacrylic acid) (PMAA) (Miyoshi *et al.*, 1996), poly(methyl vinyl ether-maleic acid) (PMVE-MAc) (Rocco *et al.*, 2001), poly(vinylphenol-*co*-methyl methacrylate) (PVPh-*co*-PMMA) (Kuo and Chang, 2001), poly(methylmethacrylate) (Osman *et al.*, 2005). Smith et al. (1959) reported that a fully amorphous inter-polymer complex resulted from complexation between PAA and PEO. Inhibition of amorphous PEO crystallization can be achieved either by anti-plasticization effects (Robeson *et al.*, 1981) or/and through formation of strong specific hydrogen bonding within the miscible polymer blends (Rocco *et al*., 2001; Kuo and Chang, 2001). Therefore, we are proposing in here that in order to stabilising the amorphous region of PEO/drug solid dispersion, a polymer-PEO blend might be viable approach in the light of well-established polymer physics theory (Flory-Huggins Theory)

The aim of this study was to investigate the potential effects of the miscibility and inter-polymer interactions in polymer blends, composed of a semi-crystalline polymer (PEO) and an amorphous polymer (Eudragit® S100), in stabilizing drug/PEO solid dispersions. In this study, HME was used to prepare PEO/Eudragit® S100 binary polymer blends and ternary systems containing the drug and the polymer blend. Celecoxib (CX), a poorly soluble non-steroidal anti-inflammatory (NSAID), was used as a model drug in this study. Eudragit® S100, an amorphous copolymer based on poly(methacrylic acid-methyl methacrylate), has been previously used as a polymeric matrix in pharmaceutical HME applications (Bruce *et al*., 2005; Schilling *et al.*, 2010a, 2010b). Eudragit® S100 has a high *Tg* and contains free carboxyl groups that can act as a proton donor or/and acceptor (Fadda *et al*., 2008). Therefore, there is a potential of miscibility and inter-polymer interactions in PEO/S100 polymer blends, which have been investigated in this study using differential scanning calorimetry (DSC), dynamic mechanical thermal analysis (DMTA) and fourier-transform infrared (FT-IR) analytical techniques.

2.0 Materials & Methods

2.1 Materials

Celecoxib (CX) was a kind gift from Hikma Pharmaceuticals (Amman, Jordan), Eudragit® S100 (MW=135000 g/mol) was donated by Evonik Röhm GmbH (Darmstadt, Germany), polyethylene oxide (MW=100,000 g/mol) (PEO 100,000), sodium chloride, and potassium bromide were purchased from Sigma-Aldrich Chemie GmbH (Poole, Dorset, England).

2.2 Methods

2.2.1 Preparation of hot-melt extrudates

Melt extrudates containing CX at 30% w/w were prepared using different ratios of PEO 100,000/Eudragit® S100 (100:0, 70:30, 50:50 and 30:70) using a co-rotating twin-screw extruder (Minilab, Thermo Electron Corporation, Stone, Staffordshire, UK) at a temperature of 150°C and a screw speed of 100 rpm. In addition, melt extrudates composed of similar ratios of binary polymeric systems of PEO/S100 without CX were prepared at similar extrusion conditions. The melt extrudates were milled by cryogenic milling using an IKA® A11 basic analytical mill (IKA® Werke GmbH, Deutschland, Germany).

2.2.2 Thermogravimetric Analysis (TGA)

The thermal stability of CX, PEO and Eudragit® S100 was studied using a TA instruments Q500 TGA (Leatherhead, UK). Ramp tests were performed at a scan speed of 10 ºC/min over a range from 20 to 500 ºC. Nitrogen was used as the purging gas during all TGA experiments.

2.2.3 Differential Scanning Calorimetry (DSC)

DSC was used to characterize the thermal properties of the drug, polymers and melt extrudates. DSC analyses were conducted using Perkin-Elmer DSC 4000 (Cambridge, UK) equipped with a refrigerated cooling system (Perkin-Elmer Intracooler-SP). Data analysis was performed using Pyris Manager software (version 10.1). Samples between 5.0 and 10.0 mg were accurately weighed and placed in crimped aluminium pans. The measurements were conducted at a heating rate of 10°C/min. The DSC was calibrated for baseline correction using empty pans, and for

temperature/enthalpy using high purity metal indium and zinc. Nitrogen was used as the purging gas at a flow rate of 20 mL/min. All analyses were performed at least in duplicate.

2.2.4 Melting point depression analysis

Miscibility within melt extruded PEO/S100 binary polymer blends has been studied using melting point depression experiment. The binary mixtures were also prepared using mortar and pestle in comparison with melt extrusion. The reduction in the melting point of the crystalline phase of PEO as a function of composition and inter-polymer interactions has been analyzed using the Nishi-Wang equation (Nishi and Wang, 1975):

$$T_m - T_{mb} = \frac{-T_m B V_2 \emptyset_1^2}{\Delta H_2} \qquad \text{Equation (1)}$$

Where *T*m and *T*mb are melting temperatures of pure crystalline polymer and the blend, respectively; the subscript *1* is identified as amorphous polymer and *2* is identified as crystalline polymer. *B* is the interaction energy density between blend components; V_2 is the molar volume of the repeating unit of the crystalline polymer; Φ_1 is the volume fraction of the amorphous polymer in the blend; and ΔH_2 is the heat of fusion of the crystalline polymer per mole of the repeating unit.

The melting points of PEO in the PEO/S100 melt extrudates (30/70-90/10 mass ratios) determined by DSC were fitted by the Nishi-Wang equation. The *B*-value was estimated by non-linear regression analysis (GraphPad Prism® version 5.04). V_2 (37.2 cm^3/mol) was calculated by summation of the volumes of the structural groups of the repeating unit of PEO (–CH_2-CH_2-O-) (Van Krevelen, 1990). The densities of PEO (1.18 g/cm^3) and Eudragit S100 (1.12 g/cm^3) were obtained from the ratios of molecular weights to molar volumes. The volume fraction of Eudragit® S100 (Φ_1) was calculated from the weight fractions and densities of the components. Seven experimental data points were used for this fit. The coefficient of determination (R^2) and randomness of the residuals were used to determine the goodness of fit.

2.2.5 Dynamic mechanical thermal analysis (DMTA)

DMTA was used in conjunction with DSC to characterize the miscibility of the binary polymer blends and the ternary systems. DMTA analyses were conducted using a

TA instruments DMA Q8000 (Leatherhead, UK). Data analysis was performed using Universal Analysis 2000 software. Approximately 30 mg of powder samples were placed inside a powder clamp used in conjunction with the dual cantilever clamp. The powder clamp is a uniquely rectangular designed stainless steel lower tray and upper cover plate assembly measuring 35x12x3.0 mm. The DMTA measurements were conducted at a heating rate of 3°C/min with an oscillatory frequency of 1 Hz. and oscillatory amplitude of 20.0 µm. All measurements were performed at least in duplicate.

2.2.6 Powder X-ray Diffractometry (PXRD)

PXRD patterns were obtained using a Rigaku Miniflex II benchtop X-ray diffractometer (Kent, UK) provided with Miniflex II Software. Samples were placed on a zero background sample holder. Cu Kα1 radiation was used as an X-ray source. The beam produced by the X-ray tube passes through a 5° soller slit and a 1.25° divergence slit. The diffraction pattern was measured using a voltage of 30kV and a current of 15mA. The angular range (3-40° 2θ) was scanned in continuous mode with a step size of 0.05° and a scan rate of 3°/min.

2.2.7 Fourier Transform Infrared (FTIR)

FTIR analyses were performed using a Fourier Transform Infrared Spectrophotometer model 4100 (FT/IR-4100) (Jasco, Japan) and Jasco Spectra Manager Version 2 Software. A small mass of each sample was mixed with dry potassium bromide (KBr) using a mortar and pestle and compressed to prepare a disk. A scanning range of 4000–400 cm^{-1} was used for all samples.

2.2.8 Stability Study

Stability studies were conducted at 40ºC and 75% RH during a four week period. Samples of milled melt extrudates were placed in open weigh boats and stored at 40 °C inside a dessicator containing a saturated sodium chloride solution. PXRD was used to qualitatively define the presence of crystalline drug and PEO content at different storage intervals.

3 Results & Discussion

3.1 Thermal stability

Thermal stability of materials is a prerequisite for HME. These materials must not degrade at, or below, the extrusion temperature used. TGA has been widely used to determine the degradation temperatures of materials and hence to assess their thermal stability prior to HME (Bruce *et al*., 2005; Zhu *et al*., 2006). TGA can determine the mass loss of material as a function of temperature, therefore this technique has often been used to identify volatile degradants. TGA ramp test of CX did not exhibit any volatile degradation prior to reaching 250°C, after which significant mass loss was detected (data not shown). As reported previously by Andrews et al. (2010b), the TGA isothermal experiments confirmed the thermal stability of CX at a temperature of 170°C. The degradation temperatures of PEO and Eudragit® S100 were determined by TGA heating ramp test at 350°C and 185°C, respectively. These significantly higher degradation temperatures than the temperature used for HME (150°C) suggest that these materials were thermally stable during HME particularly with the short residence time within the extruder <2 min and the absence of any signs of degradation from the formulations. Eudragit® S100 did lose a small percentage of total mass (~3% w/w) below a temperature of 100°C during the TGA heating ramp test, which was assumed to be due to water loss. It has been reported by Schilling et al. (2010a) that the DSC thermogram of Eudragit® S100 displayed two broad endothermic events due to evaporation of unbound water below 100°C and the thermal degradation of the polymer at 200-250°C.

3.2 Characterization of melt extrudates

DMTA has been widely used to detect the glass transition (*Tg*) of amorphous or semicrystalline polymers (Craig and Johnson, 1995; Jones, 1999). Therefore, this technique has been used in conjunction with DSC to study the miscibility of different polymer blends (Pomposo *et al*, 1996; Cascone *et al.* 1997; Bikiaris *et al*., 2004). Although both techniques give similar information, they vary significantly in their sensitivity, sample preparation and analysis (Abiad *et al*., 2010). In the DSC, the *Tg* is characterized by a change in heat capacity as a function of temperature as the material passes through the *Tg* temperature. A single compositional dependent *Tg* detected by DSC is an indication of full miscibility at a dimensional scale between 20-40 nm (Kuo and Chang, 2001). In the DMTA measurement, the ratio of the loss modulus (viscous component) to the storage modulus (elastic component) is referred

to as the loss tangent or tan delta (δ) (Brent *et al*., 1997). In general, the temperature at which the mechanical damping factor, tan delta or loss tangent, exhibits a maximum at *Tg* of the material. It has been demonstrated that DMTA is more sensitive than DSC by 1000 times in detecting the *Tg* of polymers (Bikiaris *et al*., 2004). The ability of DMTA to accurately detect changes in the moduli of polymeric systems forms the basis of the experimental determination of *Tg* temperature (Ferry, 1980). Even very weak molecular motions resulted from very small segments or parts of macromolecular chains can be detected accurately by DMTA (Wetton, 1986). The difference between the *Tg* values determined by DSC and DMTA methods is common. In DMTA, the exact position of *Tg* depends mainly on the studied frequency, whereas in DSC *Tg* depends on the used heating rate (Bikiaris *et al.*, 2004).

In our study, DMTA was used to provide more detailed and accurate information about the *Tg* of formulations and hence the miscibility within the binary and ternary systems. The DSC and DMTA thermograms of CX, PEO, Eudragit® S100 and the melt extrudates are shown in Figures 1 and 2, respectively. Table 1 summerizes the most important thermal events that have been determined from the DSC and DMTA thermograms of the drug, polymers and the melt extrudates. The heat of fusion (ΔH_f) calculated from the PEO melting transition in the DSC thermograms of the melt extrudates was used to estimate the relative degree of PEO crystallinity within the melt extrudates compared to the unprocessed PEO (Janssens *et al.*, 2008):

$$Crystallinity\ (\%) = \frac{\Delta Hf_{PEO\ in\ blend}}{(\Delta Hf_{PEO} \times w\%)} \times 100 \qquad \text{Equation (2)}$$

where the heat of fusion of unprocessed PEO was calculated to be 217.2 J/g at specified heating rate within this experiment (assumed to be 100% crystallinity). It was also used in the equation 1 for the calculation of B value for PEO/Eudragit S100 polymer blend.

It was not possible to determine the *Tg* of the amorphous domain of PEO powder either by DSC or DMTA mostly because of its low content. Melting of semicrystalline

polymers followed by solidification upon fast cooling may create larger amorphous region of the semicrystalline polymers (Prodduturi *et al*., 2005). To increase the amorphous content and ease the detection of glass transition of PEO, the unprocessed powder was heated above its melting point and then quench cooled in the DSC and DMTA instruments. The *Tg* of the amorphous PEO resulted from the quench cooled samples was determined at -38.7 °C by DMTA (tan δ peak), whereas DSC could not detect its *Tg*. Additionally, it was possible to detect the *Tg* of amorphous PEO in the melt extrudates containing pure polymer, solidified upon cooling at ambient conditions and immediately tested by DMTA (tan δ peak) (Figure 2). The increase in amorphous PEO fraction in the extruded samples comparing to the unprocessed PEO powder was due to the fast cooling after HME and subsequently the generation of more amorphous PEO region. The relatively higher *Tg* of freshly prepared pure PEO melt extrudates comparing to the *Tg* of amorphous PEO resulted from quench cooling of PEO melt, may be attributed to the significantly higher PEO crystallinity in the melt extrudates solidified upon cooling at ambient conditions (77.2%) than the melt solidified by quench cooling (62.4%). In the former process, there was more time for PEO to re-crystallize and hence greater crystallinity was formed in the sample. It has been reported that PEG 6000, which has the greatest degree of crystallinity, has the highest *Tg* among PEGs (Craig, 1995). The decrease in the amorphous content of PEO as a result of its crystallization can result in increasing the chain stiffening of the polymer, lowering its chain mobility, and consequently increasing its *Tg* (Kuo and Chang, 2001; Robeson *et al*., 1981).

PEO powder, a semicrystalline polymer, exhibits a sharp endotherm for its melting at 67.9°C in the DSC. The melting point of PEO decreased to 65.8°C after HME of the pure polymer (Figure 1). This decrease in the melting point of PEO may be related to the chemical potential decrease due to the presence of more amorphous region comparing to the unprocessed PEO powder. The PEO melting point was decreased further to 63.5°C in the PEO melt samples solidified by quench cooling attributing to the higher cooling rate.

Furthermore, in comparison to the physical mixture of PEO/S100 upon heat-cool-heat cycles, a significant decrease in the melting point was obtained for all PEO/S100 melt extrudated samples at similar w/w fractions. DSC thermograms of these sample were ploted in Figure 3 together with the Nishi-Wang equation fitted to

the PEO/S100 melt extrudated samples (Figure 3). Good agreement between the experimental and predicted Tmb was obtained for this system ($R^2 \approx 0.976$) with the B-value calculated to be -0.2691 J/cm^3. This suggested the applicability of Nishi-Wang simplified equation in assessing the miscibility and intermolecular interaction of polymer blends in molten state. More interestingly, a greater degree of melting depression, i.e. better PEO/S100 intermolecular interaction has been achieved by using the melt extrusion process in comparison to the mortar and pestle physical mixture. It also suggests that the melt extrusion may provide an optimal process for polymer blends to reach or close to the maximum interaction state of the system.

Heat-cool-heat cycles were performed on Eudragit® S100 powder samples to remove the unbound water. Eudragit® S100, an amorphous polymer, exhibits a high *Tg* which was determined to be 165.5 °C and 172.6°C, in second heat cycle from the DSC and DMTA measurements, respectively. As a result of its high *Tg* and its degradation temperature that is close to its *Tg*, it is not possible to extrude Eudragit® S100 alone without plasticization. In previous reported studies, different plasticizers have been used for HME of Eudragit® S100 formulations (Bruce *et al.*, 2005; Schilling *et al*., 2010a). In our study, PEO/S100 polymer blends were successfully extruded at a temperature significantly below the Tg of Eudragit® S100. It was not possible to prepare CX/Eudragit® S100 binary systems at temperatures below 180°C, which were dark brown indicating the possibility of Eudragit® S100 and/or CX degradation during HME. The flow property of the extrudates was poor with very long residential time indicating the high melt viscosity and consequently the high shear forces generated inside the extruder that accelerated the degradation of Eudragit® S100 and potential the CX. Lin and Yu (1999) reported using reflectance FT-IR/DSC microspectroscopy to examine the thermal stability of Eudragit® S100 that the initial reaction temperature of a 6-membered ring of cyclic anhydride degradant in Eudragit® S100 films can be very close to 180°C.

Macroscopic appearance of PEO melt extrudates can give initial indication about the PEO crystallinity and its miscibility with other polymers or drugs. Pure PEO extrudates were opaque after cooling. The opacity in the appearance of PEO melt extrudates is related to its significant content of dense crystalline regions of the polymer (Produtturi *et al*., 2005). The extruded PEO/S100 binary system at 70/30 ratio were opaque which may give an initial indication of presence of significant PEO

crystallinity. For these melt extrudates, the percentage of PEO crystallinity was calculated to be 61.1%. This indicates that a significant reduction in PEO crystallinity (16.7%) was achieved by the mixing with Eudragit® S100 at similar extrusion conditions. The melting point of PEO was further decreased to 63.5°C comparing to the PEO melting point of the extruded polymer (65.8°C). The depression in the melting point of a crystalline polymer blended with an amorphous polymer is a strong indication of their miscibility and interactions (Kuo and Chang, 2001). This occurs due to thermodynamic reasons resulted from the decrease in the chemical potential of the crystallisable polymer due to the addition of the second component. It has been reported that the melting point of PEO decreased in the PEO/poly(methyl vinyl ether-maleic acid) (PMVE-MAc) binary blends as a result of inter-polymer miscibility and hydrogen bonding (Rocco *et al.*, 2001). Increasing Eudragit® S100 content up to 50% (w/w) resulted in a more transparent PEO/S100 melt extrudates. Transparency of polymer blends is a strong indication but not a proof of miscibility. The DSC thermogram of PEO/S100 binary system of 50/50 ratio has shown a completely absence of melting endotherm from PEO and also the appearance of single Tg after HME. These results indicate that PEO is presented as an amorphous form within the PEO/S100 system at 50/50 ratio. Similar results were obtained for PEO/S100 melt extrudates of 30/70 ratio. The further reduction in PEO crystallinity within the PEO/S100 binary systems with increasing Eudragit® S100 content indicates the potential interactions between PEO and Eudragit® S100 during HME and further mixed amorphous polymer blend has been achieved. It was also reported by Chu and Wu (2000) that the reduction in PEO crystallinity in phenolic resin/PEO blends was attributed to the specific inter-polymer hydrogen bonding through the hydroxyl group of phenolic and the oxygen ether of PEO.

To further characterize the miscibility between PEO and Eudragit® S100, the *Tg(s)* of PEO/S100 binary systems were characterized by DSC and DMTA. It was not possible to detect the Tg of PEO/S100 (70/30) system in its DSC thermogram. This may be related to the presence of significant PEO crystallinity and hence the low amorphous PEO content in these melt extrudates. Conversely, DMTA thermogram exhibited a small tan δ peak at 4.93°C, which is mostly related to the Tg of PEO/S100 (70/30) system. However, a distinct single tan delta peak was detected in the DSC and DMTA thermograms of PEO/S100 (50/50) melt extrudates at -2.41 and

8.15°C, respectively. A single Tg for the PEO/S100 50/50 polymer blend between the Tg of individual components strongly suggests that this polymer blend is fully miscible blends with a homogeneous amorphous phase (Kuo and Chang, 2001). This indicates the formation of a miscible single phase after HME of PEO/S100 (50/50) system and that PEO was totally molecularly dispersed within the melt extrudates particularly with the total loss of PEO crystallinity. Previous studies on PEO binary polymer blends with different amorphous polymers reported that miscibility within the polymer blends has driven by the inter-polymer hydrogen bonding network between blend components (Miyoshi *et al*., 1996; Chu and Wu, 2000; Brus *et al*., 2000). Conversely, DMTA thermogram of PEO/S100 (30/70) system showed more than one *Tg* between the *Tg(s)* of amorphous PEO and Eudragit® S100 at tan δ peaks of 75.9, 111.2, 164.0°C, although the DSC showed only a single *Tg* at 64.8°C. These DMTA results indicate that PEO was partially miscible in the PEO/S100 (30/70) system after HME. This can highlight the importance of using DMTA as a sensitive analytical technique to detect the *Tg*(s) of the polymer blend and hence to give more accurate conclusions about the degree of miscibility between its components (Lafferty *et al*., 2002).

Although PEO was present in lower concentration in PEO/S100 (30/70) system than the 50/50 one, the 30/70 ratio was less homogeneous after HME. This non-homogeneity in PEO/S100 (30/70) system may be related to the insufficient plasticization of Eudragit® S100 by PEO (30% w/w) particularly that HME was carried out significantly lower than its *Tg*. The insufficient plasticization of polymers during HME may result in high melt viscosity and hence low mixing efficiency of the materials inside the extruder. This consequently may result in non-homogeneous polymer blend of more than one phase.

The DSC thermogram of crystalline CX showed a sharp endotherm at 163.2 °C corresponding to its melting, whereas the DMTA thermogram showed a tan δ peak at 162.2°C for the drug melting. Amorphous CX, prepared by quench cooling of the melt, exhibited a *Tg* at 58.9 and 68.6 °C in the DSC and DMTA (tan δ peak), respectively. Inclusion of CX at 30% (w/w) in PEO/S100 (30/70) system resulted in more homogeneous extrudates of single miscible phase. These effects might be related to the further plasticization effects of CX as it has significantly lower *Tg* in comparison to Eudragit® S100 and hence greater mixing efficiency.

All freshly extruded CX/(PEO/S100) ternary systems were transparent. No melting transition for PEO was detected in the DSC thermograms of the CX/(PEO/S100) 30/(50/50) and 30/(30/70) ternary systems, indicating that crystalline region of PEO was completely converted into amorphous after HME. However, a very small melting endotherm (ΔH 1.1 J/g) was detected for PEO in the DSC thermogram of CX/(PEO/S100) 30/(70/30) system indicating the presence of PEO crystalline content in melt extrudates as the PEO content increases in the polymer blends.

The observation of single Tg from DSC thermograms of all prepared CX/(PEO/S100) ternary systems would suggest the formation of a single miscible phase after HME. These DSC results were confirmed by DMTA results that also showed a single tan δ peak for these ternary systems. (They are not signle tan delta system from the DMTA other than the ratio of 50/50 PEO/S100). The Tg of these ternary systems increased with increasing Eudragit® S100 fraction as a result of its high *Tg*. The increase in the *Tg* of CX/(PEO/S100) ternary systems was in the order of 30/(70/30) > 30/(50/50) > 30/(30/70), -18.42, 7.25 and 44.47 °C (DSC) and -8.91, 37.67 and 64.18°C (DMTA, tan δ peak), respectively. Although CX/PEO (30/70) binary system does not contain Eudragit® S100, its *Tg* was higher than the *Tg* of CX/(PEO/S100) 30/(70/30) system, 0.65 and 12.30°C, determined by DSC and DMTA (tan δ peak), respectively. This higher *Tg* of CX/PEO (30/70) comparing to CX/(PEO/S100) system may be related to the significant crystallinity of PEO within the CX/PEO (30/70) melt extrudates (59.1%) i.e. lower amorphous PEO content and hence lower plasticization effects by amorphous PEO (Robeson *et al.*, 1981).

Nevertheless, no melting transition related to CX was detected in the DSC and DMTA thermograms of the CX/PEO and CX/(PEO/S100) systems. These results alone could not confirm the absence of CX crystallinity within the melt extrudates in solid state as there is a possibility that CX was dissolved within the molten PEO during the slow heating cycle of the DSC and DMTA runs. To further clarify the absence of CX crystalline form in the melt extrudates, PXRD was used to give more details and also to study their physical stability during storage.

3.3 Storage stability of melt extrudates

Figure 4 shows the PXRD spectra of crystalline CX, PEO, Eudragit® S100, and CX/PEO (30/70) physical mixture (PM). The most characteristic peaks in the PXRD

pattern of crystalline CX are located at 2θ angles of 5.6, 10.9, 15.0, 16.3, 21.7, 22.3, 27.2 and 29.7, 32.7 and 35.1º. The PXRD pattern obtained for Eudragit® S100 showed an amorphous "halo". The X-ray diffraction pattern of PEO showed distinct bragg's peaks at 2*θ* values 19.5, 22.5, 23.7, 26.5, 27.3, 35.7, and 36.5º. The X-ray pattern of the CX/PEO physical mixture (3:7), showed the bragg's peaks of PEO and crystalline CX albeit with lower intensities due to the dilution effect of CX in PEO. The most distinct non-overlapped peaks detected in the PXRD pattern of CX/PEO (30/70) physical mixture were located at 2θ 19.6 and 23.7 for PEO and at 2θ 11.3, 16.6, 22.9 and 29.9 for CX as pointed out in Figure 4. These CX and PEO distinct peaks were used as standard for the analysis of freshly prepared melt extrudates and crystal growth during the stability study.

Figures 5a-5d show the PXRD patterns of freshly prepared CX/PEO and CX/(PEO/S100) melt extrudates and after storage at 40°C and 75%RH up to 4 weeks. All the characteristic CX crystal peaks were completely absent in the PXRD patterns of the freshly prepared melt extrudates suggesting that CX crystallinity was completely lost after HME. As previously discussed, DSC and DMTA showed a single *Tg* in these systems, therefore it can be deduced that CX was molecularly dispersed within these melt extrudates. PEO crystal peaks were clearly observed in the PXRD of CX/PEO melt extrudates, whereas they were completely absent in the CX/(PEO/S100) 30/(50/50) and 30/(30/70) ternary systems. However, very small PEO crystal peaks have been detected in the PXRD pattern of CX/(PEO/S100) 30/(70/30). These PXRD results were in good agreement with the DSC results discussed earlier.

We have observed that the stability of amorphous PEO within CX/(PEO/S100) ternary systems was highly dependent on PEO/S100 ratio which significantly increases in the system containing polymer blend of 50/50 ratio than other systems. Upon storage, a rapidly recrystallization was obervered from sample CX/(PEO/S100) 30/(70/30) and 30/(30/70). The PEO crystal peaks were clearly detected in their PXRD pattern after only three days storage (Figure 5b and 5d). Interestingly, PEO remained in amorphous form within the ternary system containing PEO/S100 at 50/50 ratio without re-crystallization up to 2 weeks despite of its higher PEO content comparing to its content in the 30/(30/70) system. Only a small PEO crystal peak at 2θ 20.1 was detected after 2 weeks storage, which increased its intensity with time

(Figure 5c). These results may suggest that Eudragit® S100 polymer at PEO/S100 (50/50) ratio can provide greater stability for amorphous PEO than other PEO/S100 ratios in the ternary systems containing similar drug CX (30% w/w). This greater content of amorphous PEO may provide better carrier to accommodate drug CX and hence may lead to greater amorphous drug stability in the storage.

In comparison to ternary system, CX/PEO(30/70) solid dispersion re-crystallized rapidly. Its PXRD pattern showed distinctive CX crystal peaks after three days storage. These peaks increased in their intensities with increasing storage time (Figure 5a). In general, greater physical stability for CX was achieved by inclusion Eudragit® S100 polymer into CX/PEO solid dispersion. More interestingly, similar to the stability of amorphous PEO, the drug stability may also increase in the system containing polymer blend at 50/50 ratio. This suggests the stabilizing of amorphous PEO may result in an increase in the stability of dissolved CX molecules within the solid dispersion. Similar to CX/PEO 30/70 binary system, amorphous CX re-crystallized rapidly from the CX/(PEO/S100) 30/(70/30) and 30/(30/70) systems after 3 days storage but with lower CX crystal peaks number and intensities. Furthermore, no CX crystal peaks were detected in the PXRD pattern of the ternary system of 30/(50/50) up to 4 weeks under stress conditions (the duration of the stability study). It should be noted that, due to the high miscibility between CX and molten polymer PEO during the extrusion (under low temperature condition), most of dissolved drug CX should be distributed within the amorphous region of polymer PEO. Therefore, we propose that, this superior storage stabilization of CX in this system may be attributed to the stabilization of amorphous domain of PEO using amorphous polymer Eudragit S100, which consequently resulted in the stabilizing the drug dissolved within it.

3.4 The effect of amorphous polymer Eudragit S100

It has been previously demonstrated that physical stabilization of amorphous solid dispersions may be related to antiplasticization effects by blending with polymers with higher *Tg*. Formation of miscible systems (solid molecular dispersions) of single *Tg* that is significantly higher than the *Tg* of amorphous drugs can result in enhanced stability by decreasing their molecular mobility (Van den Mooter *et al.*, 2001). Although the *Tg* of the CX/(PEO/S100) 30/(50/50) system was significantly lower

than the *Tg* of CX (PEO/S100) 30/(30/70), the stability of both amorphous PEO and CX were significantly greater. This means that the anti-plasticization effects achieved by increasing Eudragit S100 amount in the ternary systems was not the predominant mechanism in this physical stabilization of amorphous PEO and CX. Another reported mechanism of stabilizing amorphous solid dispersions is through formation of strong specific drug/polymer interactions (Huang *et al*., 2008). Certain types of molecular association are needed to achieve crystallization, so disruption of the hydrogen bond patterns in amorphous compounds would be useful in the physical stabilization of amorphous phases. Thus by targeting the proton donor and/or acceptor groups in the amorphous drug to interact with the polymer can result in inhibition of crystallization of the amorphous form (Tang *et al*., 2002). CX/PEO (30/70) solid solution was relatively unstable comparing to the ternary systems containing similar drug amount. This means that CX/PEO intermolecular interactions, if exist, has no significant role in such stabilization of CX in the ternary systems. Increasing polymer/drug ratio may increase the strength of hydrogen bonding between the drug and polymer, as this makes the polymer functional groups are more available for interactions with drug molecules. Ozeki et al. (1997) reported that the strength of hydrogen bonding increased with increasing PEO content in flurbiprofen/PEO solid dispersions. Additionally, the strength of hydrogen bonding increased significantly with increasing polyvinylpyrrolidone (PVP) concentration in felodipine solid dispersions (Karavas *et al.,* 2006). If any intermolecular interactions between CX and Eudragit® S100 formed during HME, they would be stronger and more significant in CX/(PEO/S100) 30/(30/70) system than 30/(50/50) as it has higher Eudragit® S100/CX ratio. Therefore, drug/polymer interactions might not be the main reason behind the stabilization of amorphous CX within the CX30/(50/50) system. These findings highlight the importance of investigating the role of inter-polymer interactions in such stabilization, which has not been explored in pharmaceutical literature before.

The high miscibility between PEO and Eudragit® S100 after HME suggests that specific inter-polymer interactions might have been formed, which mostly stabilized the amorphous region of PEO and consequently the drug molecules dissolved within the inter-polymer network. It has been shown that PEO crystallization was retarded and even inhibited by adding the amorphous poly(vinylphenol-co-

methylmethacrylate) (PVPh-co-PMMA) copolymer through formation of hydrogen bonding between the hydroxyl group of PVPh-co-PMMA and the ether oxygen of PEO (Kuo and Chang, 2001).

Infrared spectroscopy has been proven a highly effective means of investigating specific interactions between polymers. FTIR studies were conducted in order to characterize the type of the inter-polymer interactions within the melt extrudates. The chemical structure of PEO consists of repeat units of polyethylene oxide monomers (–CH_2-CH_2-O-). PEO can act as a proton acceptor through the oxygen ether of the ethylene oxide monomer (Robeson *et al*., 1981), which may interact with the proton donor group of Eudragit® S100, the carboxylic acid group, during HME. The FTIR spectrum of PEO showed a triplet peak in the region of 1000-1200 cm^{-1} (1054, 1095, and 1150 cm^{-1}), which were related to the stretching vibration of C-O-C bond (Socrates, 1994). The intensity and shape of the C-O-C stretching mode of PEO with the significant decrease in their positions were indicative of formation of strong specific hydrogen bonding between PEO and PMVE-MAc (Rocco *et al.*, 2001). Unfortunately, the FTIR spectrum of Eudragit® S100 exhibited strong peaks at this region due to the stretching vibrations from the C-O-C of the ester group of melthylmethacrylate monomer (Socrates, 1994). Additionally, amorphous CX exhibited bands of significant intensities in this region (Gupta and Bansal, 2005). Therefore, it was difficult to make definite conclusions about any significant changes in the stretching vibration bands of the oxygen ether of PEO that might have been occurred after HME due to the overlapping from the CX and Eudragit® S100 peaks. The broad absorption band located in the region of 3157-3678 cm^{-1} in the FTIR spectrum of PEO was due to the stretching vibration of the O-H bonded to C-H. However, the stretching band of OH group of Eudragit® S100 was higher in its intensity and located in a wider region 3046-3727 cm^{-1} (centred at 3435 cm^{-1}). In the binary polymer blends and ternary systems, the stretching broad band of PEO was overlapped by the relatively more intense band of the O-H bonded to C=O group of methacrylic acid of Eudragit® S100. After HME, this band has been shifted toward lower frequencies (red shift) in the spectra of both binary and ternary polymer blends comparing to corresponding physical mixtures. This red shifting may be attributed to the formation of inter-polymer hydrogen bonding interactions between the OH group of Eudargit® S100 (proton donor) and the oxygen ether of PEO (proton acceptor).

Interestingly, more significant shift in the position of the OH stretching band of Eudragit® S100 has been occurred after HME of the binary polymer blend at 50/50 ratio comparing to the other polymer blends suggesting stronger hydrogen bonding (Figure 6a). Similarly, the ternary system containing a polymer blend of 50/50 ratio exhibited further red shifting (3426 cm^{-1}) in the position of the OH group from Eudragit® S100 than the other ternary systems, which was located at 3431 cm^{-1} and 3433 cm^{-1} in the spectra of CX/(PEO/S100) (30/(70/30) and 30/(30/70), respectively.

For the lower wavenumber range in the FTIR, the stretching vibration band of C=O group of the free carboxyl groups in methylmethacrylic acid of Eudragit® S100 was detected at 1705 cm^{-1}. The very low intensity of this band was mostly due to the overlapping from the more intense stretching vibration band of the esterified carbonyl group (1731 cm^{-1}), particularly that the ratio of the free carboxyl groups to the ester groups in Eudragit® S100 is approximately 1:2. It was not possible to detect this band in the spectra of the PEO/S100 physical mixture samples due to the dilution effect. Interestingly, after HME of the binary polymer blends, it was possible to detect two separate small stretching bands related to the C=O of the carboxyl groups of Eudragit® S100 (Figure 6b). The red shifts in one of these bands toward lower frequencies may be attributed to the formation of hydrogen bonding between the C=O of the carboxyl groups of Eudragit® S100 and the hydroxyl group (OH) of PEO. Conversely, blue shifts toward higher frequencies have been occurred to the corresponding band. These blue shifts might be resulted from the weakness or disruption of the intra- or/and intramolecular interactions between the C=O bonded to O-H within Eudragit® S100 molecules as a result of the hydrogen bonding formation. Furthermore, the intensities of these bands in PEO/S100 melt extrudates increases in the order 50/50 > 70/30 > 30/70. Interestingly, this order was in a good agreement with the degree of red shifting that has been recorded in the position of OH stretching band of Eudragit® S100 after HME. Increasing PEO content in PEO/S100 binary blend resulted in increasing inter-polymer interactions significantly from 30% to 50% PEO then the strength of hydrogen bonding decreased as a result of further increase in PEO and the significant PEO crystallinity within the melt extrudates. Kuo and Chang (2001) have reported similar trend that, the inter-polymer hydrogen bonding interactions between PEO and PVPh-co-PMMA were largely depended on the PEO content within the binary polymer blends.

In our study, the intensities of C=O stretching band of the Eudragit® S100 in the binary polymer blend of 50/50 was the greatest among other systems. This gives further evidence of formation of stronger hydrogen bonding within the melt extrudates of PEO/S100 at ratio 50/50 than the other ratios. An increase in the band intensity can give a more reliable indication of the hydrogen bonding than the red shift of stretching frequency (Lutz and Jacob, 1996). Similar findings have been deduced from the FTIR spectra of the ternary systems that, the intensities of the peaks related to the stretching vibration of C=O of the carboxyl groups of Eudragit® S100 increased after HME particularly in the ternary system containing PEO/S100 (50/50). It clearly suggests the existence of stronger inter-polymer hydrogen bonding at this ratio comparing to other ternary systems. These results indicate that the strong inter-polymer hydrogen bonding that has been formed between the carboxyl groups of Eudragit® S100 and the oxygen ether of PEO in the binary polymer blend still presented in the ternary system at ratio of 50/50. We propose that, the strong inter-polymer network was mostly responsible for the greatest physical stabilization of amorphous PEO within the ternary system of 30/(50/50) ratio, and consequently the predominant mechanism in stabilizing the molecularly dispersed CX molecules.

4.0 Conclusions

This study highlighted the importance of inter-polymer interactions in stabilizing amorphous solid dispersions of poorly soluble drug system. The high miscibility between PEO and Eudragit® S100 at specific ratio and the stabilization effects of on amorphous PEO resulted in enhanced the storage stability of amorphous CX solid dispersion within the inter-polymeric complexity. DMTA analytical technique was efficient in detecting the *Tg* of amorphous PEO and consequently in studying the miscibility within the prepared systems. FTIR studies gave evidence of formation of strong inter-polymer hydrogen bonding particularly in the system containing polymer blend of 50/50 ratio. This was in good agreement with PXRD studies that showed greater stabilization in this system comparing to other systems. In this study, the inter-polymer interactions showed higher effects than the antiplasticization effects by Eudragit®S100 in stabilizing the amorphous PEO and consequently the dissolved CX molecules. This suggests that these inter-polymer interactions were the predominant mechanism behind such stabilization.

References

Abiad, M., G., Gonzalez, D., C., Mert, B., Campanella, O., H., Carvajal, M., T. 2010. A novel method to measure the glass and melting transitions of pharmaceutical powders. *International Journal of Pharmaceutics*, 396, 23-29.

Abu Diak, O.; Jones, D.; Andrews, G. An Investigation into the Dissolution Properties of Celecoxib Melt Extrudates: Understanding the Role of Polymer Type and Concentration in Stabilizing Supersaturated Drug Concentrations. *Molecular pharmaceutics* 2011, *8,* 1362-1371.

Abu Diak, O., Jones, D.S., Andrews, G.P., 2012. Understanding the performance of melt-extruded poly(ethylene oxide)-bicalutamide solid dispersions: Characterisation of microstructural properties using thermal, spectroscopic and drug release methods. Journal of Pharmaceutical Sciences, 101, 200-213.

Albers, J., Alles, R., Matthée, K., Knop, K., Nahrup, J., S., Kleinebudde, P. 2009. Mechanism of drug release from polymethacrylate-based extrudates and milled strands prepared by hot-melt extrusion. *European Journal of Pharmaceutics and Biopharmaceutics*, 71 (2): 387-394.

Andrews, G., P., Abu-Diak, O., Jones, D., S. 2010a. Physicochemical characterization of hot-melt extruded bicalutamide-polyvinylpyrrolidone solid dispersions, *Journal of Pharmaceutical Sciences,* 99 (3):1322-1335.

Andrews, G., P., Abu-Diak, O., Kusmanto, F., Hornsby, P., Hui, Z., Jones, D., S. 2010b. Physicochemical characterization and drug-release properties of celecoxib hot-melt extruded glass solutions, *Journal of pharmacy and pharmacology*, 62(11), 1580-1590.

Bikiaris, D., Prinos, J., Botev, M., Betchev, C., Panayiotou, C. 2004. Blends of polymers with similar glass transition temperatures: A DMTA and DSC study. Journal of applied polymer science, 93, 726-735.

Brent Jr., J., L., Mulvaney, S., J., Cohen, C., Bartsch, J., A. 1997. Viscoelastic properties of extruded cereal melts. J. Cereal Sci., 26, 313-328.

Breitenbach, J. 2002. Melt extrusion: from process to drug delivery technology. *European Journal of Pharmaceutics and Biopharmaceutics*, 54: 107-117.

Bruce, L., D., Shah, N., H., Malick, A., W., Infeld, M., H., McGinity, J., W. 2005. Properties of hot-melt extruded tablet formulations for the colonic delivery of 5-aminosalicylic acid. *European Journal of Pharmaceutics and Biopharmaceutics*, 59: 85-97.

Brus, J., Dybal, J., Schmidt, P., Kratochvil, J., Baldrain, J. 2000. Order and mobility in polycarbonate-poly(ethylene oxide) blends studied by solid-state NMR and other techniques. *Macromolecules*, 33: 6448-6459.

Cascone, M., G., Polacco, G., Lazzeri, L., Barbani, N. 1997. Dextran/poly(acrylic acid) mixtures as miscible blends. *Journal of Applied Polymer Science*, 66, 2089-2097.

Chiou, W., L., Riegelman, S. 1971. Pharmaceutical applications of solid dispersion systems. *Journal of Pharmaceutical Sciences*, 60: 1281-1302.

Chu, P., P., Wu, H., D. 2000. Solid state NMR studies of hydrogen bonding network formation of novolac type phenolic resin and poly(ethylene oxide) blend. *Polymer*, 41: 101-109.

Craig, D., Q., M. 2002. The mechanisms of drug release from solid dispersions in water-soluble polymers. *International Journal of Pharmaceutics*, 231: 131-144.

Craig, D., Q., M., Johnson, F., A. 1995. Pharmaceutical applications of dynamic mechanical thermal analysis. *Thermochimica Acta*, 248, 97-115.

Craig D., Q., M. 1995. A review of thermal methods used for the analysis of the crystal form, solution thermodynamics and glass transition behaviour of polyethyleneglcols. *Thermochimica Acta*, 248,189-203.

Craig, D., Q., M. 1990. Polyethylene glycols and drug release. *Drug Development and Industrial Pharmacy*, 16: 2501-2526.

Crowley, M., M., Zhang, F., Repka, M., A., Thumma, S., Upadhye, S., B., Battu, S., K. 2007. Pharmaceutical applications of hot-melt extrusion: Part I. *Drug Development and Industrial Pharmacy*, 33: 909-926.

Crowley, M., M., Fredersdorf, A., Schroeder, B., Kucera, S., Prodduturi, S., Repka, M., A., McGinity, J., W. 2004. The influence of guaifenesin and ketoprofen on the properties of hot-melt extruded polyethylene oxide films, *European Journal of Pharmaceutical Sciences*, 22, 409-418

Dubin, C., H. 2005. Formulation Frustrations. *Drug Delivery Technology*, 5: 30-34.

Ferry, J., D. 1980. Viscoelastic properties of polymers. John Wiley and Sons, New York.

Fadda, H., M., Hernández, M., C., Margetson, D., N., McAllister, S., M., Basit, A., W., Brocchini, S., Suárez, N. 2008. The molecular interactions that influence the plasticizer dependent dissolution of acrylic polymer films. *Journal of Pharmaceutical Sciences*, 97(9): 3957-3971

Gupta P., Bansal A., K. 2005. Molecular interactions in celecoxib–PVP–meglumine amorphous system. *Journal of Pharmacy and Pharmacology*, 57:303–310.

Hancock, B., C., Zografi, G. 1997. Characteristics and significance of the amorphous state in pharmaceutical systems. *Journal of Pharmaceutical Sciences*, 86: 1-12.

Huang, J., Wigent, R., J., Schwartz, J., B. 2008. Drug–polymer interaction and its significance on the physical stability of nifedipine amorphous dispersion in microparticles of an ammonio methacrylate copolymer and ethylcellulose binary blend. *Journal of Pharmaceutical Sciences*, 97 (1): 251-262.

Janssens, S., De Armas, H., N., Roberts, C., J., Van den Mooter, G. 2008. Characterization of ternary solid dispersions of itraconazole, PEG 6000, and HPMC 2910 E5, *Journal of Pharmaceutical Sciences*, 97(6), 2110-2120

Jones, D., S. 1999. Dynamic mechanical analysis of polymeric systems of pharmaceutical and biomedical significance. *International Journal of Pharmaceutics*, 179, 167-178

Karavas, E., Ktistis, G., Xenakis, A., Georgarakis, E. 2006. Effect of hydrogen bonding interactions on the release mechanism of felodipine from nanodispersions

with polyvinylpyrrolidone. *European Journal of Pharmaceutics and Biopharmaceutics*, 63: 103-114.

Kuo, S., W., Chang, F., C. 2001. Miscibility and hydrogen bonding in blends of poly(vinylphenol-co-methylmethacrylate) with poly(ethylene oxide). *Macromolecules*, 34: 4089-4097.

Lafferty, S., V., Newton, J., M., Podczeck, F. 2002. Dynamic mechanical thermal analysis studies of polymer films prepared from aqueous dispersion. *International Journal of Pharmaceutics*, 235, 107-111.

Lakshman, J., P., Cao, Y., Kowalski, J., Serajuddin, A.,T. 2008. Application of melt extrusion in the development of a physically and chemically stable high-energy amorphous solid dispersion of a poorly water-soluble drug. *Molecular Pharmaceutics*, 5 (6): 994-1002.

Leuner, C., Dressman, J. 2000. Improving drug solubility for oral delivery using solid dispersions. *European Journal of Pharmaceutics and Biopharmaceutics*, 50: 47-60.

Li, L., AbuBaker, O., Shao, Z., J. 2006. Characterization of poly(ethylene oxide) as a drug carrier in hot-melt extrusion. *Drug Development and Industrial Pharmacy*. 32: 991-1002.

Lin, S., Yu, H. 1999. Thermal stability of methacrylic acid copolymers of Eudragits L, S, and L30D and the acrylic acid polymer of carbopol. *Journal of Polymer Science*, 37,13, 2061-2067.

Lindenberg, M., Kopp, S., Dressman, J., B. 2004. Classification of orally administered drugs on the World Health Organization Model List of Essential Medicines according to the biopharmaceutics classification system. *European Journal of Pharmaceutics and Biopharmaceutics*, 58: 265-278.

Lipinski, C., A., Lombardo, F., Dominy, B., W., Feeney, P., J. 2001. Experimental and computational approaches to estimate solubility and permeability in drug discovery and development setting. *Advanced Drug Delivery Reviews*, 46: 3-26.

Lutz, B., Jacob, J., van der Maas. 1996. Vibrational spectroscopic characteristics of =C---H. . O and N---H. . π interaction in crystalline N-(2,6-dimethylphenyl)-5-methylisoxazole-3-carboxamide. *J. Vib. Specrosc.*, *12*, 197–206.

Marsac, P., Konno, H., Taylor, L., S. 2006. A comparison of the physical stability of amorphous felodipine and nifedipine systems, *Pharmaceutical Research*, 10: 2306-2316.

Matsumoto, T., Zografi, G. 1999. Physical properties of solid molecular dispersions of indomethacin with poly(vinylpyrrolidone) and poly(vinylpyrrolidone-co-vinyl-acetate) in relation to indomethacin crystallization. *Pharmaceutical Research*, 16: 1722-1728.

Miller, D., A., DiNunzio, J., C., Yang, W., McGinity, J., W., Williams, R., O. 2008. Targeted intestinal delivery of supersaturated itraconazole for improved oral absorption. *Pharmaceutical Research*,25(6):1450-1459.

Miyoshi, T., Takegoshi, K., Hikichi, K. 1996. Higher-resolution solid-state ^{13}C nuclear magnetic resonance study of polymer complex: poly(methacrylic acid)/poly(ethylene oxide). *Polymer*, 37: 11-18

Osman, Z., Ansor, N., M., Chew, K., W., Kamarulzaman. 2005. Infrared and conductivity studies on blends of PMMA/PEO based polymer electrolytes. Ionics, 11: 431-435.

Ozeki, J., Y., Yuasa, H., Kanaya, Y. 1997. Application of the solid dispersion method to the controlled release of medicine. IX. Difference in the release of flurbiprofen from solid dispersions with poly(ethylene oxide) and hydroxypropylcellulose and the interaction between medicine and polymers. *International Journal of Pharmaceutics*, 155: 209–217.

Pomposo, J., A., de Juana, R., Múgica, A., Cortázar, M. 1996. Binary poly(ethylene oxide)/poly(methyl methacrylate-co-ethyl methacrylate) blends: miscibility predictions from model compound mixtures *vs* experimental phase behaviour. *Macromolecules*, 29, 7038-7046.

Prodduturi, S., Manek, R., V., Kolling, W., M., Stodghill, S., P., Repka, M., A. 2005 Solid-state stability and characterization of hot-melt extruded poly(ethylene oxide) films. *Journal of Pharmaceutical Sciences*, 94 (10): 2232-2245.

Robeson, L., M., Hale, W., F., Merriam, N., C. 1981. Miscibility of Poly (hydroxyl ether) of Bisphenol A with water-soluble polyethers. *Macromolecules,* 14: 1644-1650.

Sarnes, A.., Kovalainen, M., Hakkinen, M.R., Laaksonen, T., Laru, J., Kiesvaara, J., Ilkka, J., Oksala, O., Ronkko, S., Jarvinen, S., Hirvonen, K., Peltonen, L. 2014. Nanocrystal-based per-oral itraconazole delivery: Superior in vitro dissolution enhancement versus Sporanox® is not realized in in vivo drug absorption. Journal of Controlled Release, 180, 109-116.

Serajuddin, A., T., M. 1999. Solid dispersion of poorly water-soluble drugs: early promises, subsequent problems, and recent breakthroughs. *Journal of Pharmaceutical Sciences*, 88 (10): 1058-1066.

Schachter, D., M., Xiong, J., Tirol, G., C. 2004. Solid state NMR perspective of drug–polymer solid solutions: a model system based on poly(ethylene oxide). *International Journal of Pharmaceutics* 28: 89–101.

Schilling, S., U., Lirola, H., L., Shah, N., H., Malick, A. W., McGinity, J., W. 2010a. Influence of plasticizer type and level on the properties of Eudragit S100 matrix

pellets prepared by hot-melt extrusion. *Journal of Microencapsulation*, 27(6): 521-532

Schilling, S., U., Shah, N., H., Waseem, M., A., McGinity, J., W. 2010b. Properties of melt extruded enteric matrix pellets. *European Journal of Pharmaceutic and Biopharmaceutics*, 74(2): 352-361.

Smith, K., L., Winslow, A., E., Peterson, D., E. 1959. Association reactions for poly(alkylene oxides) and polymeric poly(carboxylic acids). *Ind. Eng. Chem.*, 51: 1361-1364

Tang, X., C., Pikal, M., J., Taylor, L., S. 2002. A spectroscopic investigation of hydrogen bond patterns in crystalline and amorphous phases in dihydropyridine calcium channel blockers. *Pharmaceutical Research*, 19: 477-483.

Tian Y, Booth J, Meehan E, Jones D.S., Li S, Andrews G.P., 2013. Construction of Drug-Polymer Thermodynamic Phase Diagrams Using Flory-Huggins Interaction Theory: Identifying the Relevance of Temperature and Drug Weight Fraction to Phase Separation within Solid Dispersions. Mol Pharm 10:236-248.

Tian Y, Caron, V., Jones D.S., Healy, A.M., Andrews G.P., 2014. Using Flory-Huggins phase diagrams as a pre-formulation tool for the production of amorphous solid dispersions: A comparison between hot-melt extrusion and spray drying. Journal of Pharmacy and Pharmacology, 66, 256-274.

Van den Mooter, G., Wuyts, M., Blaton, N., Busson, R., Grobet, P., Augustijns, P., Kinget, R. 2001. Physical stabilization of amorphous ketoconazole in solid dispersions with polyvinylpyrrolidone K25. *European Journal of Pharmaceutical Sciences*, 12: 261-269.

Van Krevelen, D., W. Volumetric properties. In: Van Krevelen D., W., editor. Properties of polymers: Their correleation with chemical structure; their numerical estimation and prediction from additive group contributions, 3rd edn. Amsterdam: Elsevier Science Publishers. pp 71-88

Wetton, R., E., in Developments in Polymer Characterization; Dawkins, J., V., Ed.; Elsevier Applied Science: London.

Zhang, F., McGinity, J., W. 1999. Properties of sustained-release tablets prepared by hot-melt extrusion. Phamaceutical Development and Technology, 4, 241-250.

Zhu, Q., Taylor, L., S., Harris, M., T. 2010. Evaluation of the microstructure of semicrystalline solid dispersions. *Molecular Pharmaceutics*, 7(4): 1291-1300.

Zhu, Y., Mehta, K., A., McGinity, J., W. 2006. Influence of plasticizer level on the drug release from sustained release film coated and hot-melt extruded dosage forms. *Pharmaceutical Development and Technolology*, 11, 285–294.

Table Captions

Table 1. The most important thermal events determined from the DSC and DMTA thermograms of CX, PEO, Eudragit® S100 and the melt extrudates.

Table 1.

	Tm (°C)	ΔH (J/g)	Tg (°C)	
			DSC	DMTA (Tan δ peak)
CX	163.2	84.0	58.9	68.6
PEO powder	67.9	217.2	ND	-38.7
PEO HME	65.8	167.5	ND	-30.0
Eudragit® S100			165.5	172.6
CX/PEO				
30/70		89.8	0.65	12.3
PEO/S100				
30/70	ND	ND	64.8	75.9, 111.2, 164.0
50/50	ND	ND	-2.41	8.15
70/30	63.5	92.8	5.70	4.93
CX/(PEO/S100)				
30/(30/70)		ND	44.5	64.2
30/(50/50)		ND	7.3	37.7
30/(70/30)		1.07	-18.4	-8.9

ND : PEO enthalpy could not be detected i.e. complete loss of PEO crystallinity (totally amorphous).
Values in brackets represent the PEO % crystallinity calculated based on equation (1).

Figure Captions

Figure 1. DSC thermograms of CX, PEO, Eudragit® S100 and the melt extrudates (↙ represents the *Tg* position).

Figure 2. DMTA thermograms of CX, PEO, Eudragit® S100 and the melt extrudates (↙ represents the *Tg* position).

Figure 3. Fit of experimental data to Nishi-Wang equation: Tmb of PEO in Eudargit® S100 system prepared by physic mixture (◆) melt extrudates obtained from experimental data (■); predicted by Nishi-Wang equation (–).

Figure 4. PXRD patterns of CX, Eudragit® S100, PEO and CX/PEO PM (30/70).

Figure 5. PXRD patterns of freshly prepared melt extrudates and after storage at 40°C and 75% RH up to 4 weeks. a) CX/PEO (30/70); b) CX/(PEO/S100) 30/(70/30); c) 30/(50/50); d) 30/(30/70).

Figure 6. FTIR spectra of PEO/S100 binary polymer blends a) 3000-4000 cm^{-1}; b) 1600-1800 cm^{-1}.

Figure 1

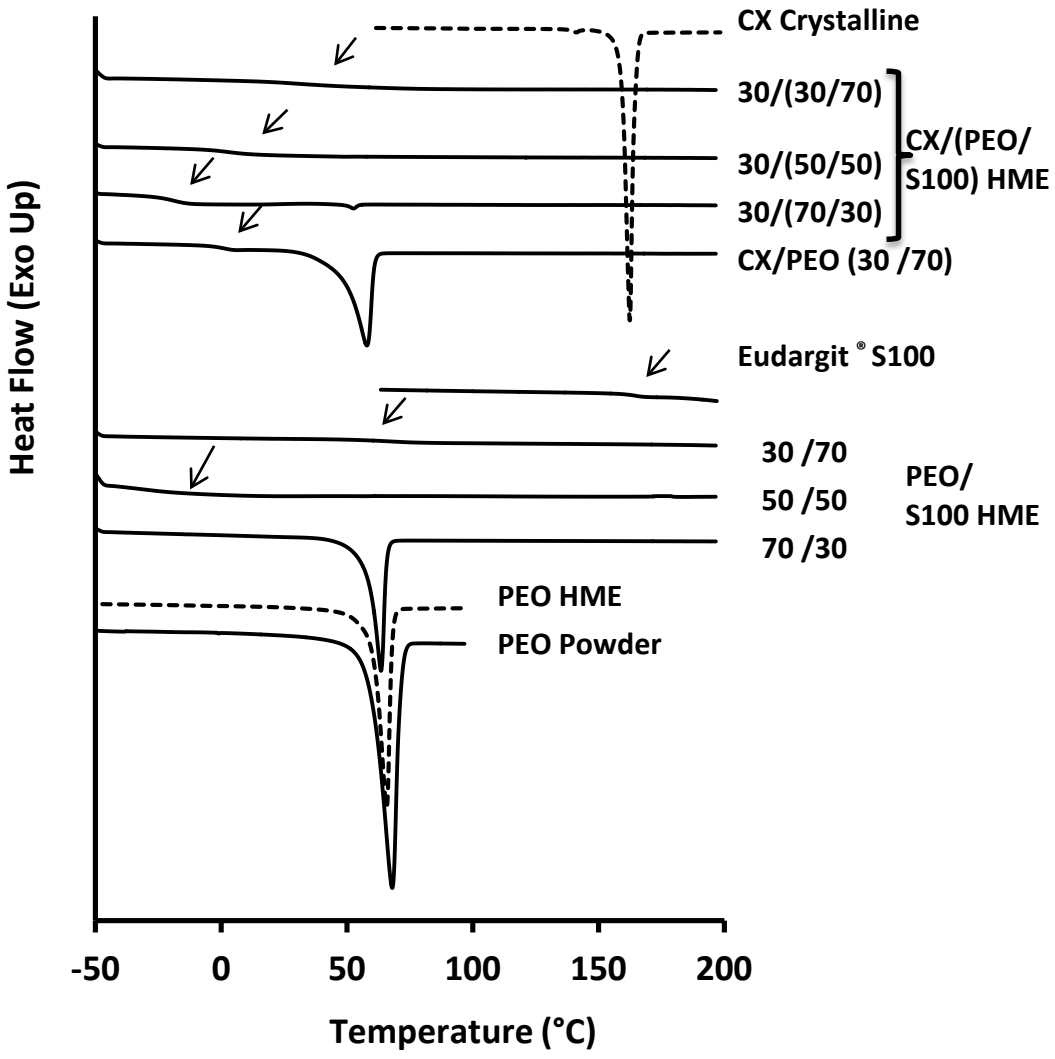
CX Crystalline
30/(30/70)
30/(50/50)
30/(70/30)
CX/(PEO/ S100) HME
CX/PEO (30 /70)
Eudargit ® S100
30 /70
50 /50
70 /30
PEO/ S100 HME
PEO HME
PEO Powder
Heat Flow (Exo Up)
-50
0
50
100
150
200
Temperature (°C)

Figure 2

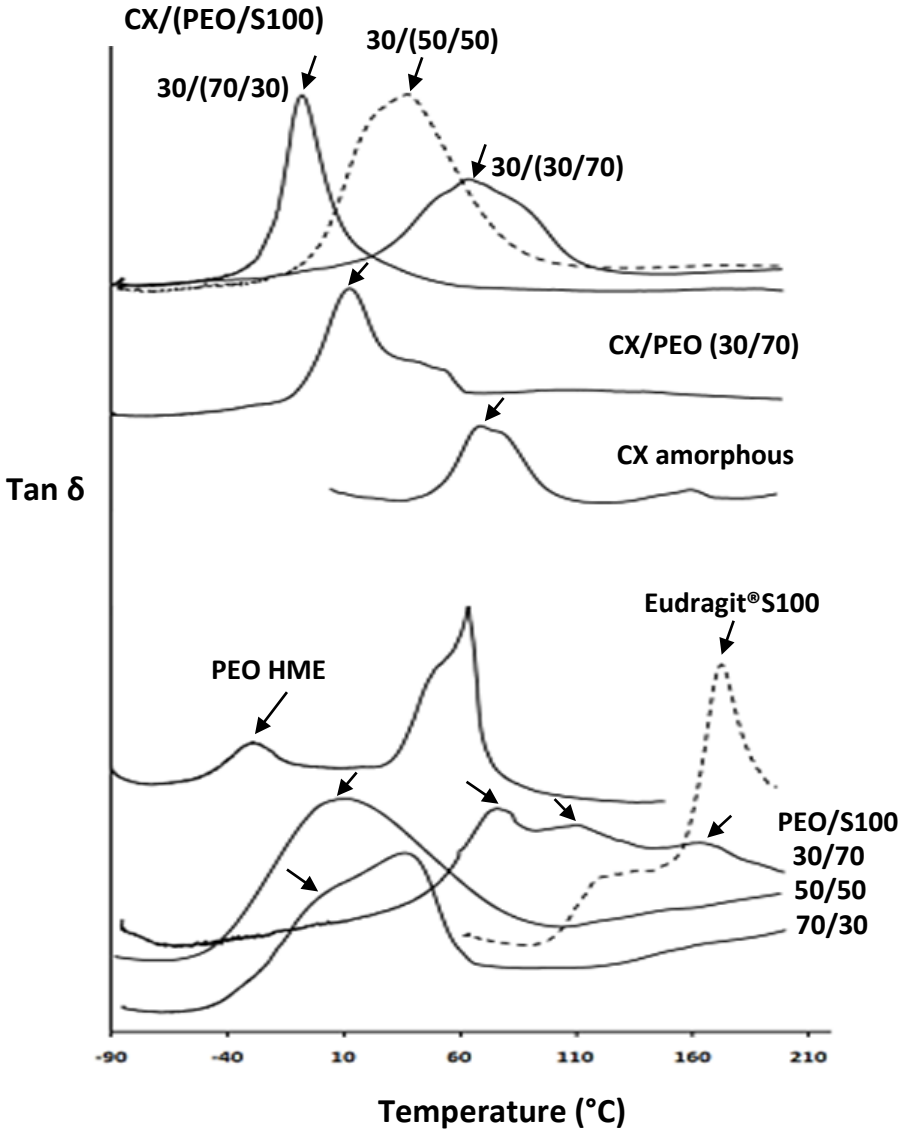
CX/(PEO/S100)
30/(50/50)
30/(70/30)
30/(30/70)
CX/PEO (30/70)
CX amorphous
Tan δ
Eudragit®S100
PEO HME
PEO/S100
30/70
50/50
70/30
-90
-40
10
60
110
160
210
Temperature (°C)

Figure 3

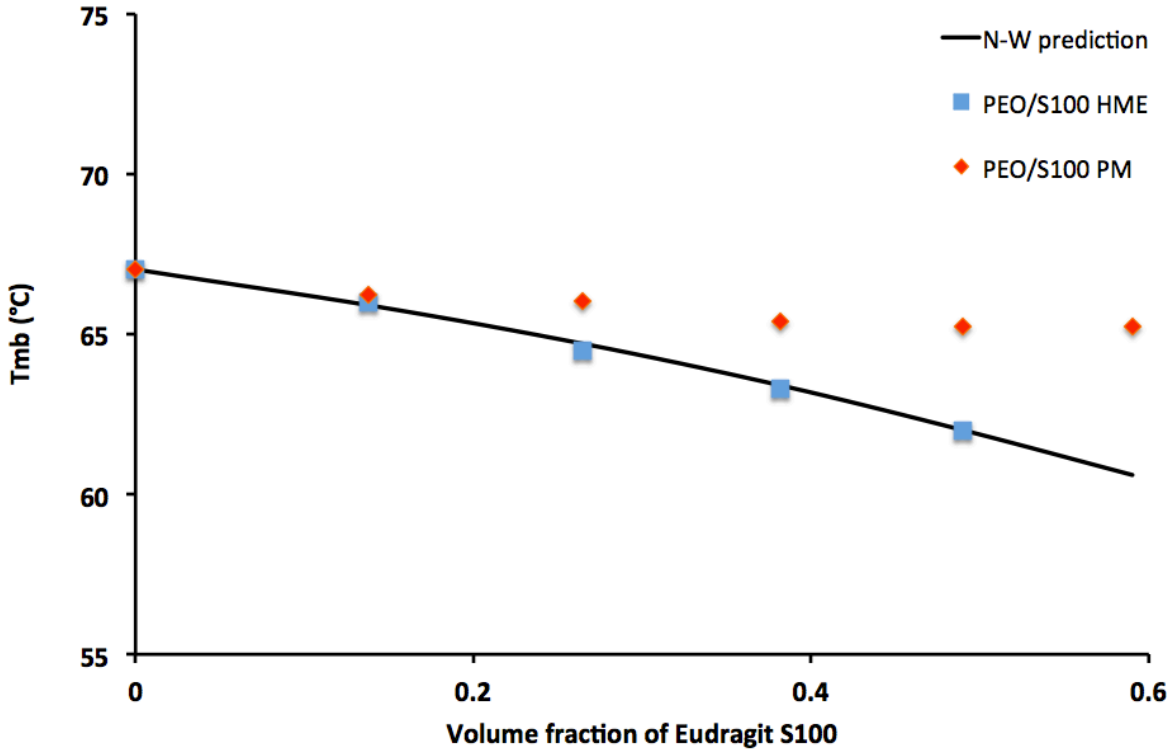
75
70
65
60
55
Tmb (°C)
0
0.2
0.4
0.6
Volume fraction of Eudragit S100
N-W prediction
PEO/S100 HME
PEO/S100 PM

Figure 4

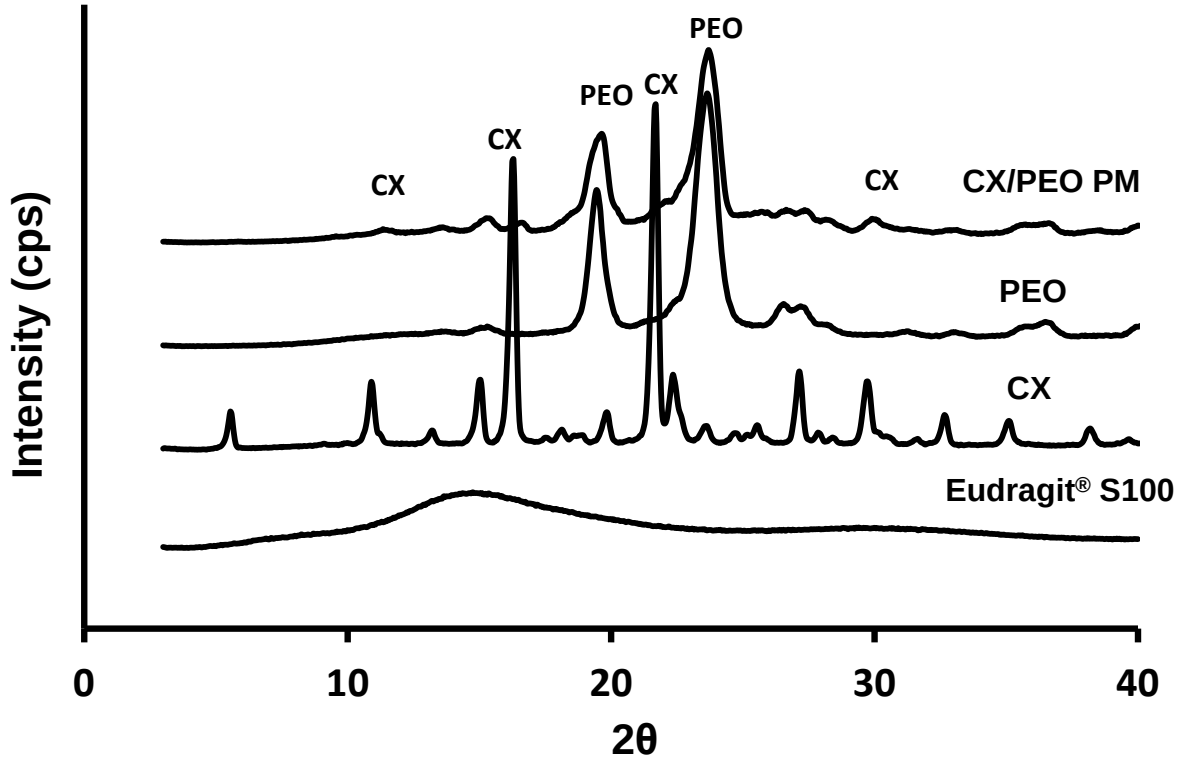
PEO
PEO
CX
CX
CX
CX
CX/PEO PM
PEO
CX
Eudragit® S100
Intensity (cps)
0
10
20
30
40
2θ

Figure 5a

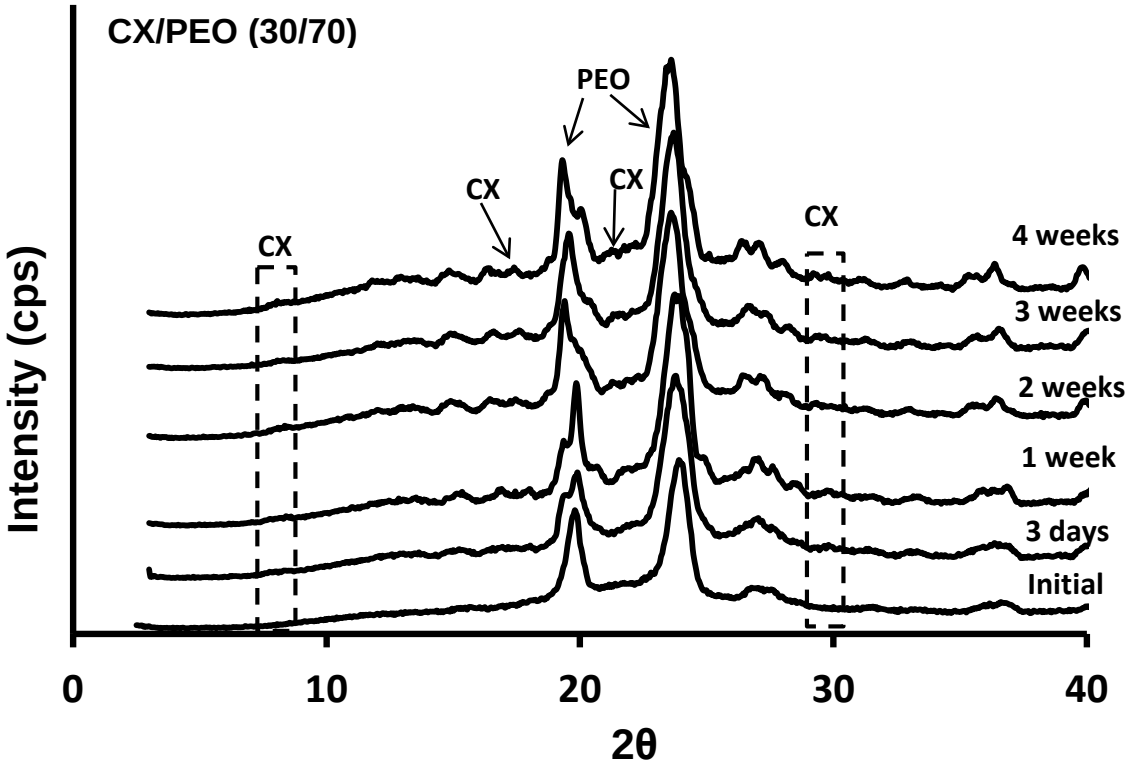
CX/PEO (30/70)
PEO
CX
CX
CX
CX
4 weeks
3 weeks
2 weeks
1 week
3 days
Initial
Intensity (cps)
0
10
20
30
40
2θ

Figure 5b

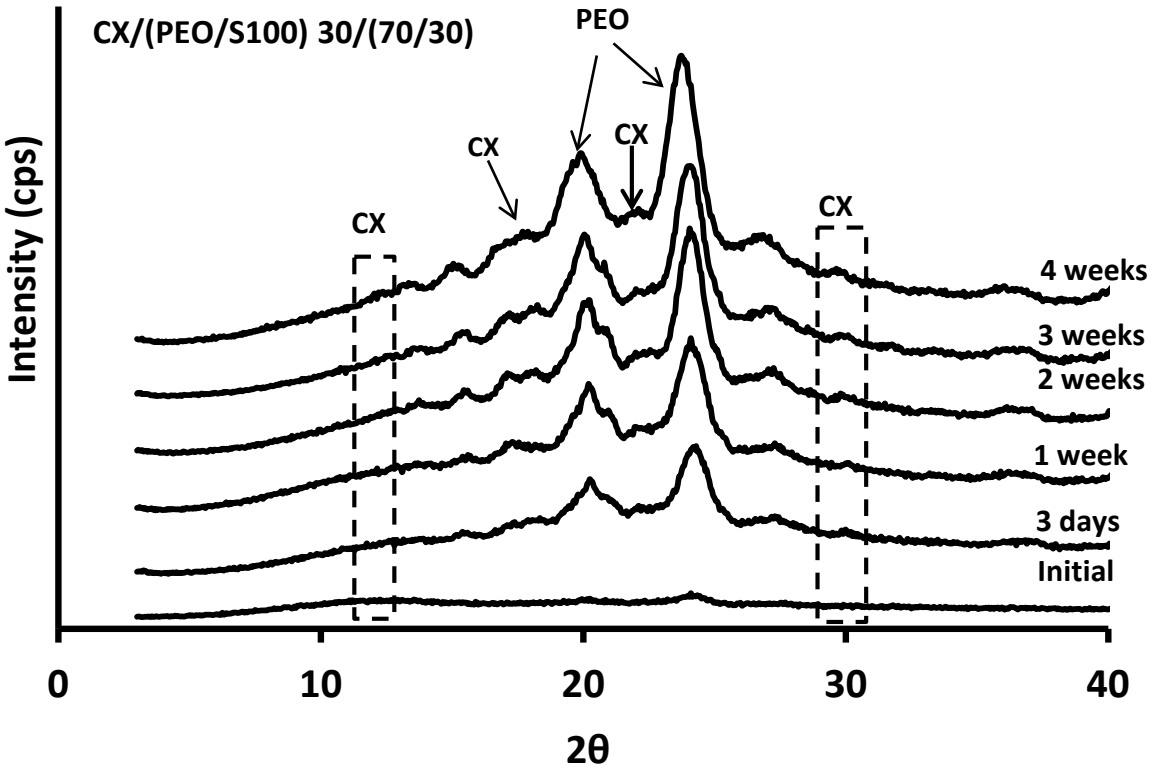
CX/(PEO/S100) 30/(70/30)
PEO
CX
CX
CX
CX
Intensity (cps)
4 weeks
3 weeks
2 weeks
1 week
3 days
Initial
0
10
20
30
40
2θ

Figure 5c

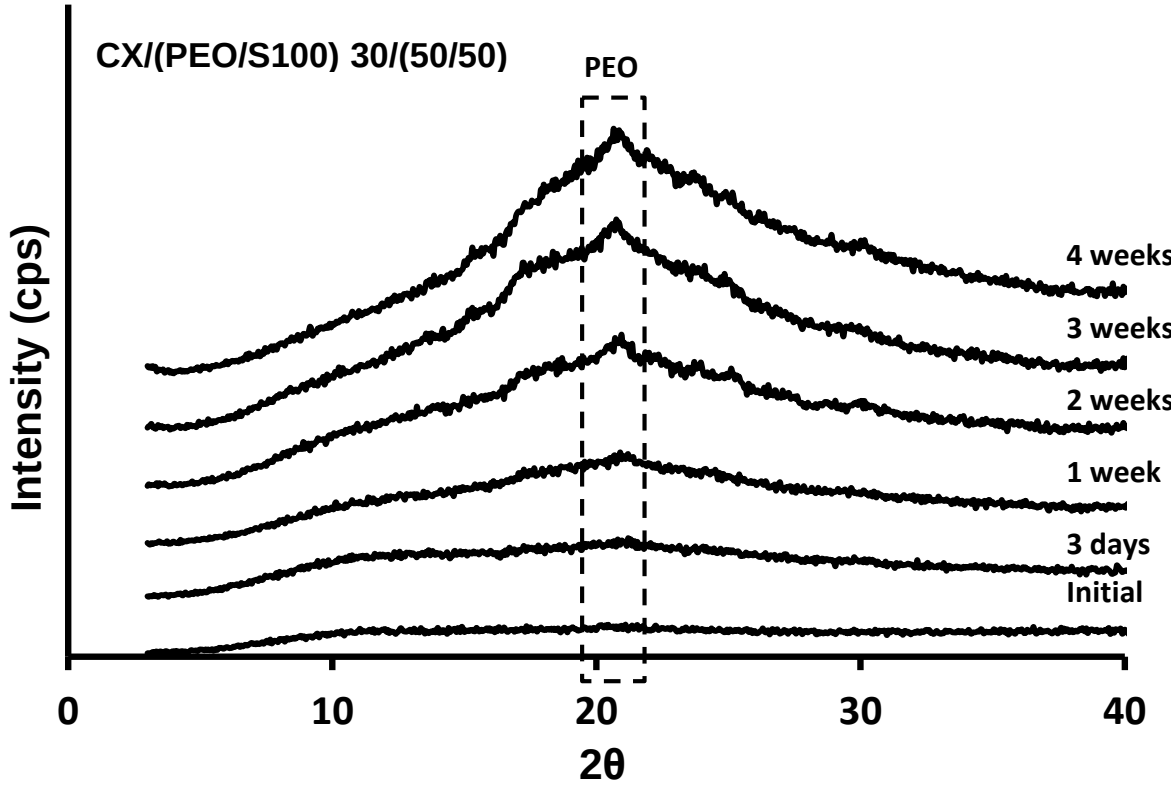
CX/(PEO/S100) 30/(50/50)
PEO
Intensity (cps)
4 weeks
3 weeks
2 weeks
1 week
3 days
Initial
0
10
20
30
40
2θ

Figure 5d

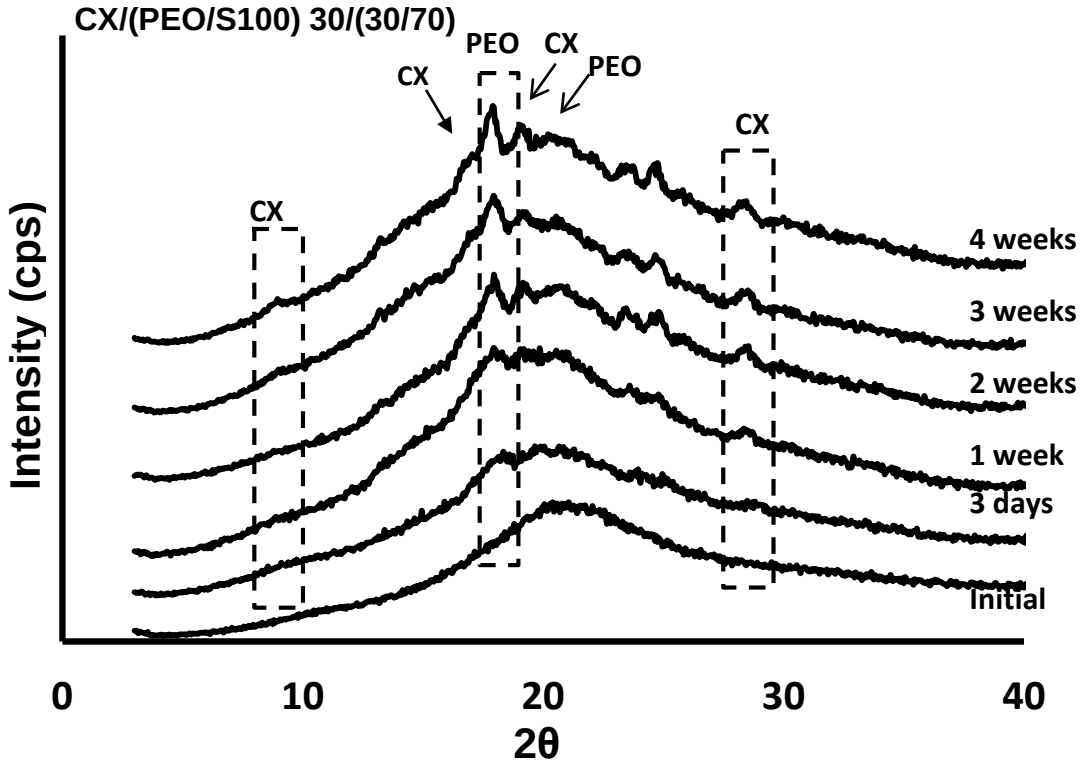
CX/(PEO/S100) 30/(30/70)
PEO
CX
CX
PEO
CX
CX
4 weeks
3 weeks
2 weeks
1 week
3 days
Initial
Intensity (cps)
0
10
20
30
40
2θ

Figure 6a (it is hard to see the shifts and intensity difference)

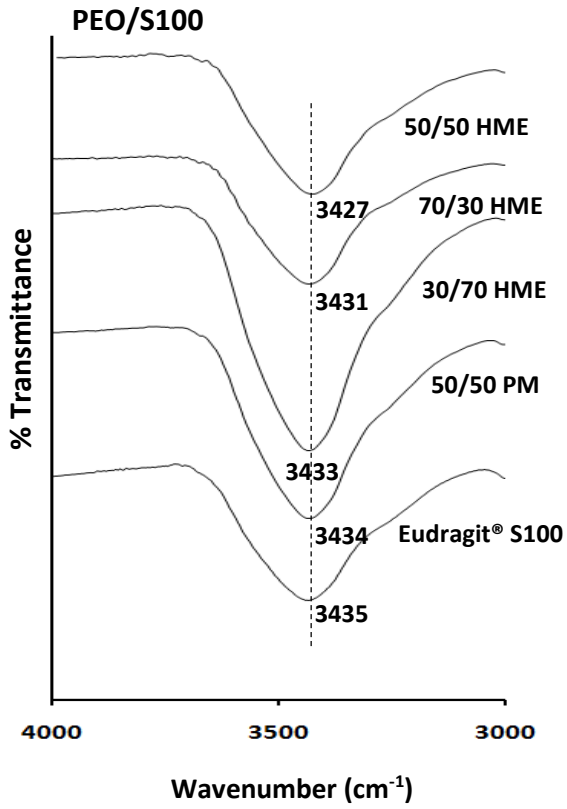

Figure 6b (hard to see the shoulders in 1700+ and intensity difference)